

# Synthesis of silver nanotubes by electroless deposition in porous anodic aluminium oxide templates

Shu-Hong Zhang, Zhao-Xiong Xie,\* Zhi-Yuan Jiang, Xin Xu, Juan Xiang, Rong-Bin Huang and Lan-Sun Zheng

State Key Laboratory for Physical Chemistry of Solid Surfaces & Department of Chemistry, Xiamen University, Xiamen 361005, China. E-mail: zxxie@xmu.edu.cn; Fax: +86-592-2183047

Received (in Cambridge, UK) 8th December 2003, Accepted 17th March 2004

First published as an Advance Article on the web 5th April 2004

An electroless deposition method has been employed for the synthesis of silver nanotubes using porous anodic aluminium oxide as templates, by which high-yield silver nanotubes with length over ten microns have been synthesized.

Nanostructures with hollow interiors have been the focus of much current research due to their potential uses in many areas. Such materials may serve as extremely small containers for encapsulation, as host materials to load catalysts, and as small templates to build other nanostructural systems, *etc.*<sup>1–3</sup> Owing to their unique properties in comparison with their bulk counterparts,<sup>4</sup> noble metals of hollow nanostructures are of particular interest. Great effort has been devoted to the synthesis of such one-dimensional (1D) nanomaterials and there have appeared some successful examples for the synthesis of various noble metal materials with hollow nanostructures.<sup>3,5,6</sup> To our knowledge, however, synthesis of silver nanotubes has not been reported yet. In this communication, we report a high-yield synthesis of silver nanotubes by electroless deposition in porous anodic aluminium oxide (AAO) templates, a very simple, low-cost and green chemical method.

The AAO templates with ordered nanopore arrays used in our work have a thickness of about 15  $\mu\text{m}$ .<sup>7</sup> Diameters of the nanochannels in the templates range from 25 nm to 60 nm. Before the electroless deposition, the AAO templates were first kept under low pressure ( $\sim 9.9$  Torr) for more than 8 hours. Then the AAO templates were immersed in a freshly prepared electroless bath solution (pH = 8–9) containing silver complex ( $4.25 \times 10^{-3}$  M  $\text{Ag}(\text{NH}_3)_2^+$ ) and a reductant consisting of  $2.27 \times 10^{-2}$  M glucose and  $2.67 \times 10^{-3}$  M tartaric acid. After 24 hours at the temperature of 15–20  $^\circ\text{C}$ , AAO templates were taken out from the plating bath and immersed in de-ionized water to remove the reactants, and then the templates were dissolved in 4 M NaOH for more than 12 hours. After dissolving the AAO templates, the raw products were centrifuged and rinsed with de-ionized water several times. Finally, black solids were collected and ultrasonically dispersed in ethanol to get a suspended solution for further analysis.

Figs. 1a and 1b show the typical transmission electron microscope (TEM, JEM-100CX) images of the products. As can be seen, the products consist of a tubular 1D nanostructure. The nanotubes spread uniformly over a narrow range of diameters, being about 25 to 60 nm for the outer diameters and 10–30 nm for the inner diameters. The outer diameters correspond well to the pore size of the AAO templates used, and it is found the outer diameters can be adjusted by choosing other AAO templates of different pore size. The nanotubes may grow over ten microns long with open tops. The short nanotubes could be straight, while the long nanotubes are usually bent. Further evidence of the nature of the nanotubes comes from the high-resolution transmission electron microscope (HRTEM, Tecnei F30) images. Figs. 1c and 1d show the HRTEM images of the walls of nanotubes. In Fig. 1c, the fringe spacing along the perpendicular direction to the long axis of the tube was measured to be 0.21 nm; while that along the long axis of the tube was measured to be 0.29 nm. The former corresponds to the interplanar (100) distance; while the latter corresponds to the (110) distances of Ag (fcc). Thus the long axis of the tube is along the (110) direction. In Fig. 1d, the fringe spacing of 0.24 nm was measured along the direction perpendicular to the long axis of the tube. This corresponds well to the interplanar (111) distance.

Therefore, the as-prepared nanotubes are Ag nanotubes. It should be pointed out that the Ag nanotubes are unstable and collapse in a few seconds under the irradiation of electron beam in the TEM chamber, making it difficult to take high quality TEM images. The collapse of Ag nanotubes is due to the re-crystallization of Ag caused by the heat generated from electron beam irradiation, since the silver nanotube may suffer from a high strain.

The presence of Ag nanotube can be further confirmed by using X-ray diffraction (XRD). Fig. 2 shows the XRD pattern of the as-prepared Ag nanotube. All the peaks can be attributed to the *fcc* Ag (JCPDS Card No. 4–783) and are obviously broadened, owing to the nanosize of the Ag crystals.

Fig. 3a shows the UV-visible absorption spectroscopy of as-prepared products. There is an absorption peak around 390 nm, which is caused by the surface plasmon resonance of one-dimensional Ag nanostructures.<sup>8,9</sup> The position of the absorption peak is in agreement with the diameter of the Ag nanotubes. In Fig. 3b, a fluorescence spectrum of Ag nanotubes from the ethanol suspension was presented, which shows a peak at 354 nm. Luminescence of noble metal nanoclusters was previously assigned to the radiative recombination of Fermi level electrons and sp- or d-band holes.<sup>10</sup> We speculate that the same basic mechanism also works for the fluorescence of Ag nanotubes observed here.

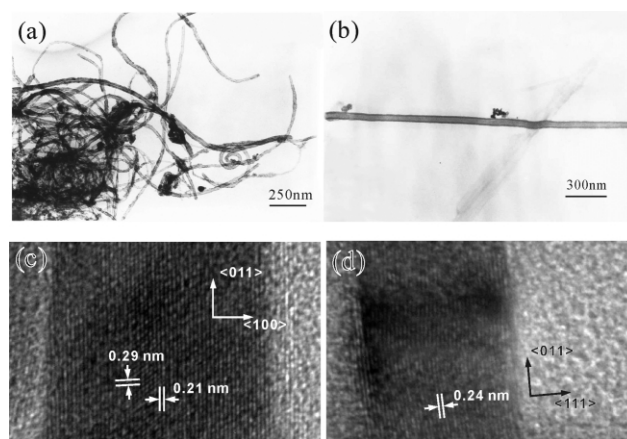


Fig. 1 (a, b) Typical TEM images of silver nanotubes synthesized by electroless deposition in AAO templates. (c, d) HRTEM images of the wall of silver nanotubes; the left sides are the core of the tube for their relatively dark color.  $\langle hkl \rangle$  represents the  $\langle hkl \rangle$  or its equivalent directions.

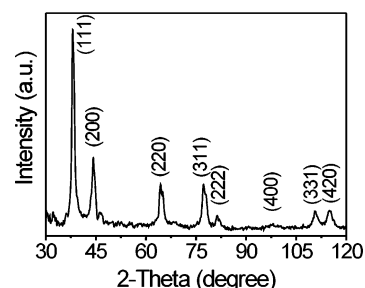


Fig. 2 The XRD pattern of the as-prepared silver nanotubes.

Previous reports showed that a large quantity of alumina nanotubes/nanowires was obtainable by etching porous alumina membranes in an aqueous NaOH solution at room temperature.<sup>11</sup> Thus special attention has to be paid not to mistake alumina nanotubes for deposited metal nanotubes. In the present work, about 5 times the calculated volume of NaOH solution was used to dissolve the corresponding amount of AAO templates and the dissolving time was kept long enough (more than 12 hours).

Template-directed synthesis of metal 1D nanostructures may be the most promising route in terms of cost and productivity. Owing to its hexagonally ordered and nearly parallel porous structures, AAO has caused a great deal of excitement as template in the synthesis of various nanorods.<sup>12–16</sup> Some metal tubular structures in micron or nanometer scale have also been successfully synthesized.<sup>17–20</sup> The key to the formation of these tubular structures in templates was believed to be due to the presence of “molecular anchors” on the pore wall.<sup>19</sup> In the present work, no external “molecular anchors” were introduced.

The reaction used for the formation of Ag nanotubes by the electroless deposition in templates can be viewed as being borrowed from the well-known Tollens’ test in sugar chemistry, where the silver ion is reduced to metallic silver, which deposits in the form of a mirror on the wall of the test tube.<sup>21</sup> The detailed mechanism of the formation of the nanotubes could be very complicated,<sup>22</sup> but we proposed that it may follow a self-catalytic reduction route as described below. First, the pore wall of AAO templates might have some defect (active) sites, serving as original nucleation sites for the reduction of silver complex ions. Once the nuclei are formed, the silver species serves as the precursor or catalyst for the subsequent reduction of silver ions and the silver grows in the form of tubes owing to the geometrical confinement of the nano-channels. We infer that the subsequent reduced silver atoms deposit onto the top of the tubes, resulting in 1D growth of the tubes. The HRTEM images show that the long axis is along the  $\langle 110 \rangle$  direction and the side walls are made of (111) and (100) planes. This growth direction is the same as found for some Ag nanowires.<sup>9</sup> As it is known that the (110) facet has a relatively high chemical potential, the growth rate on this facet should be much faster than that on any other facets, which results in the preferential growth of Ag nanotubes along the  $\langle 110 \rangle$  direction. The (111) and (100) surfaces are the most and the next most stable surfaces, respectively. Hence these surfaces form the ending walls of the nanotubes. We believe that the preferential crystal growth of silver is a controlling factor for the growth of Ag nanotubes. This accounts for the observation that nanotubes might grow out of the templates. The scanning electron microscope (SEM) image of a cross section of a template after the electroless deposition for 2 hours (relatively short deposition time) shows that some nanotubes have already grown out of the templates as marked by arrows in Fig. 4.

It should be pointed out that to get a high yield of Ag nanotubes, the surfaces of the AAO templates and the vessels should be kept clean to avoid undesired reactions. Moreover, AAO templates should be kept under low pressure ( $\sim 9.9$  Torr) for several hours ( $> 8$  hours) to drive out gases trapped inside the pores prior to the

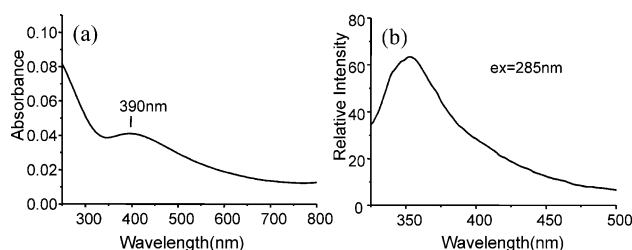


**Fig. 3** (a) UV-vis absorption spectra of an ethanol suspension of silver nanotubes. (b) Room temperature fluorescence emission spectra of silver nanotubes in ethanol at the exciting wavelength of 285 nm.

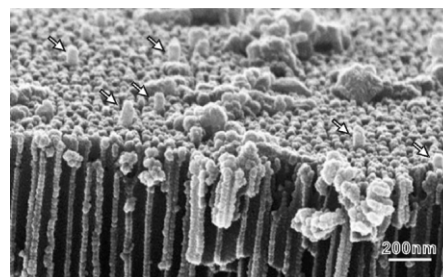


**Fig. 4** SEM image of a cross section of a template filled with silver nanotubes, which shows some silver nanotubes have grown out of the AAO template.

electroless deposition because the solutions enter small pores by the capillary effect. The pH value is another key factor to obtain high quality nanotubes. To avoid corrosion of AAO templates in strong alkali or strong acid, the resulting pH value of the electroless bath has to be adjusted to around 8 or 9.

In summary, high yield silver nanotubes with diameters corresponding to the AAO template pore sizes and of length up to tens of microns have been successfully synthesized using electroless deposition. This work should be of interest as a successful example of the fabrication of silver nanotubes and the electroless deposition in templates may be applied to the synthesis of nanotubes of other metals.

This work is supported by the NSF of China (Grant No. 20021002, 20173046), the Ministry of Science and Technology of China (Grant No. 2001CB610506, 2002CCA01600), the NSF of Fujian Province (Grant No. E0310004) and the Fok Ying-Tung Educational Foundation.

## Notes and references

- 1 F. Caruso, *Adv. Mater.*, 2001, **13**, 11.
- 2 M. Sauer, D. Streich and W. Meier, *Adv. Mater.*, 2001, **13**, 1649.
- 3 Y. G. Sun, B. T. Mayers and Y. N. Xia, *Nano Lett.*, 2002, **2**, 481.
- 4 D. Sarkar and N. J. Halas, *Phys. Rev. E*, 1997, **56**, 1102.
- 5 Y. G. Sun, B. Mayers, T. Herricks and Y. N. Xia, *Nano Lett.*, 2003, **3**, 955.
- 6 V. P. Menon and C. R. Martin, *Anal. Chem.*, 1995, **67**, 1920.
- 7 The AAO templates were prepared using a one-step anodizing process. In brief, the high-purity ( $> 99.99\%$ ) aluminium foil was anodized for one hour in 4% oxalic acid electrolytes with 40 V voltage. The temperature of the electrolytes was kept constant at 20 °C.
- 8 S. Kapoor, *Langmuir*, 1998, **14**, 1021.
- 9 Y. G. Sun, B. Gates, B. Mayers and Y. N. Xia, *Nano Lett.*, 2002, **2**, 165.
- 10 J. P. Wilcoxon, J. E. Martin, F. Parsapour, B. Wiedenman and D. F. Kelley, *J. Chem. Phys.*, 1998, **108**, 9137.
- 11 Z. L. Xiao, C. Y. Han, U. Welp, H. H. Wang, W. K. Kwok, G. A. Willing, J. M. Hiller, R. E. Cook, D. J. Miller and G. W. Crabtree, *Nano Lett.*, 2002, **2**, 1293.
- 12 G. Sauer, G. Brehm, S. Schneider, K. Nielsch, R. B. Wehrspohn, J. Choi, H. Hofmeister and U. Gosele, *J. Appl. Phys.*, 2002, **91**, 3243.
- 13 X. Y. Zhang, L. D. Zhang, Y. Lei, L. X. Zhao and Y. Q. Mao, *J. Mater. Chem.*, 2001, **11**, 1732.
- 14 H. Zeng, M. Zheng, R. Skomski, D. J. Sellmyer, Y. Liu, L. Menon and S. Bandyopadhyay, *J. Appl. Phys.*, 2000, **87**, 4718.
- 15 Y. Peng, H. L. Zhang, S. L. Pan and H. L. Li, *J. Appl. Phys.*, 2000, **87**, 7405.
- 16 X. Y. Zhang, B. D. Yao, L. X. Zhao, C. H. Liang, L. D. Zhang and Y. Q. Mao, *J. Electrochem. Soc.*, 2001, **148**, G398.
- 17 C. R. Martin, *Adv. Mater.*, 1991, **3**, 457.
- 18 C. R. Martin, L. S. Van Dyke, Z. H. Cai and W. B. Liang, *J. Am. Chem. Soc.*, 1990, **112**, 8976.
- 19 C. J. Brumlik and C. R. Martin, *J. Am. Chem. Soc.*, 1991, **113**, 3174.
- 20 R. V. Parthasarathy and C. R. Martin, *Chem. Mater.*, 1994, **6**, 1627.
- 21 A. Streitwieser, Jr. and C. H. Heathcock, *Introduction to Organic Chemistry*, Macmillan, New York, 1985, p. 710.
- 22 J. Belloni, M. Mostafavi, H. Remita, J.-L. Marignier and M.-O. Delcourt, *New J. Chem.*, 1998, 1239.